

# Berezinskii-Kosterlitz-Thouless crossover in a photonic lattice

Eran Small, Rami Pugatch, and Yaron Silberberg

*Department of Physics of Complex Systems, Weizmann Institute of Science, Rehovot 76100, Israel*

(Received 24 May 2010; published 7 January 2011)

We show that a periodic two-dimensional (2D) photonic lattice with Kerr nonlinearity exhibits a Berezinskii-Kosterlitz-Thouless (BKT) crossover associated with a vortex-unbinding transition. We find that averaging over random initial conditions is equivalent to Boltzmann thermal averaging with the discrete nonlinear Schrödinger Hamiltonian. By controlling the initial randomness we can continuously vary the effective temperature. Since this Hamiltonian is in the 2D  $XY$  universality class, a BKT transition ensues. We verify this prediction using experimentally accessible observables and find good agreement between theory and simulations. This opens the possibility of experimental access to interesting phase transitions known in condensed matter using nonlinear optics.

DOI: [10.1103/PhysRevA.83.013806](https://doi.org/10.1103/PhysRevA.83.013806)

PACS number(s): 42.65.Wi, 05.70.Fh, 03.75.Lm, 75.30.Kz

## I. INTRODUCTION

The celebrated Berezinskii-Kosterlitz-Thouless (BKT) transition describes a unique phase transition in two dimensions; whereas long-range order is forbidden in the thermodynamic limit, but quasi-long-range order associated with a diverging correlation length prevails for all temperatures below the BKT transition temperature  $T_c$  [1,2]. Nelson and Kosterlitz predicted a universal jump in the superfluid stiffness at  $T_c$  [3], which was subsequently measured in a landmark experiment by Bishop and Reppy [4] using cold  $^4\text{He}$ . The BKT transition was also manifested in coupled superconductor islands [5] and is closely related to the algebraic decay of x-Ray Bragg peaks of a smectic- $A$  liquid crystal [6]. Recently, a BKT crossover was observed using ultracold Rb atoms in a two-dimensional optical trap [7].

In the field of nonlinear optics, the nonlinear Schrödinger equation (NLSE) and its discrete version (DNLS) are successfully employed to describe the propagation of light in a Kerr nonlinear medium [8–10]. These equations are mathematically equivalent to the equation that describes the evolution of a weakly interacting Bose-Einstein condensate in the mean-field approximation [11]. In particular the discrete version describes coupled BEC's in an optical lattice [12,13]. While an optical analogy between nonlinear light satisfying the NLSE and massive bosons in the superfluid phase was noted before [14], no attempt was made to devise an optical analog to the BKT phase transition.

Here we report a method to create an effective temperature in certain optical setups and employ this method to create an optical analog to the BKT transition as a function of the effective temperature in a particular realization—a nonlinear two-dimensional waveguide array. We show that using a standard optical setup and observables we can directly observe the transition. Our method relies on the nonintegrability of the underlying Hamiltonian and thus can be generalized to other optical setups.

## II. NONLINEAR PHOTONIC LATTICE PROPAGATION

Consider light propagating through a nonlinear periodic two-dimensional (2D) square array of weakly coupled waveguides. The propagation follows the  $2+1$  DNLS equation

where the propagation direction  $z$  plays the role of time:

$$i \frac{d\psi_i}{dz} = -J \sum_{j(i)} \psi_j + \gamma |\psi_i|^2 \psi_i \quad (1)$$

where  $\psi_i$  is the complex amplitude of the mode in the  $i$ th lattice site,  $J$  is the coupling coefficient to the nearest neighbors, the sum  $\sum_{j(i)}$  indicates a sum over all nearest neighbors of the  $i$ th lattice site, and  $\gamma$  is the nonlinear coefficient.

We focus on the case where light is injected into the array with uniform amplitudes  $|\psi_i| = \psi_0 = \text{const}$ . We set both the tunneling energy  $J$  and the input amplitude  $\psi_0$  to 1 so the normalized nonlinear coefficient  $\Gamma = \gamma \psi_0^2 / J$  and the normalized propagation distance is  $\tilde{z} = Jz$  where  $\gamma \psi_0^2$  is the nonlinear self-energy term. With this normalization, the input intensities are all uniform with normalized  $|\psi_i| = 1$ .

Equation (1) describes the equations of motion derived from the DNLS Hamiltonian. The normalized form of this Hamiltonian is

$$\hat{H}(\psi_i) = -\frac{1}{2} \sum_{(i,j)} (\psi_i \psi_j^* + \psi_i^* \psi_j) + \frac{1}{2} |\Gamma| \sum_{i=1}^N I_i^2, \quad (2)$$

where  $i$  and  $j$  are lattice indices that run over all  $N$  sites in the 2D array, the sum  $\sum_{(i,j)}$  is a sum over all nearest neighbors in the array, and  $I_i = |\psi_i|^2$  is the intensity at the  $i$ th lattice site. The sign of the Hamiltonian is chosen to make sure its eigenenergies are bounded from below.

## III. DEFINING THERMALIZATION AND EFFECTIVE TEMPERATURE

Having introduced the equations of motion and the underlying Hamiltonian, we now turn to explain how the nonintegrability of the DNLS Hamiltonian allows us to generate an effective temperature. The DNLS Hamiltonian has only two integrals of motion, the total intensity  $I = \hat{N}(\psi_i) = \sum_i |\psi_i|^2$  and the total energy  $E = \hat{H}(\psi_i)$ . Hence the motion through phase space composed of all the modes  $\psi_i$  that conserve both  $E$  and  $I$  is ergodic. It is therefore possible to define a Boltzmann weight  $e^{-\beta[\hat{H}(\psi_i) - \mu \hat{N}(\psi_i)]}$  that will enable us to replace any thermodynamic time-averaged quantity by an ensemble average [15]. To be more specific,

the time average of  $X(t)$  is  $\langle X \rangle_t = (1/t) \int_0^t dt' X(t')$ , which is, for large  $t$ 's, equal to the ensemble average  $\langle X \rangle_B = \int d[\psi_i] (1/Z) e^{-\beta[\hat{H}(\psi_i) - \mu \hat{N}(\psi_i)]} X(\psi_i)$ , where  $Z$  is the normalization factor (also the partition function),  $\beta$  is the inverse effective temperature, which is the Lagrange multiplier that fixes the average energy to the conserved value  $E$ , and  $\mu$  is a second Lagrange multiplier (chemical potential) that fixes the average total intensity to  $I$ . Note that the time  $t$  is equivalent to the propagation distance  $z$ , so the optical analog of a time average is averaging over the optical output at varying (long) propagation distances.

A more practical implementation would be to work at a fixed distance. For that purpose we define another type of averaging, namely, averaging over random initial conditions. Consider an experiment where the input light field  $\psi_i$  injected into each of the waveguides is experimentally controlled. Define a thermalization distance  $z_{\text{thermal}}$  which is the distance after which information about the initial condition is lost due to ergodicity. Then if the overall propagation distance  $z_{\text{tot}}$  is larger than  $z_{\text{thermal}}$ , averaging over initial conditions becomes equivalent to averaging over the propagation distance which in turn is equivalent to Boltzmann-weighted ensemble averaging.

To summarize, due to the nonintegrability of the DNLS Hamiltonian, averaging over random-phase initial conditions after a fixed propagation length is equivalent to thermal averaging with an effective temperature. This temperature is defined as the inverse of the Lagrange multiplier coupled to the Hamiltonian.

In order to evaluate the effective temperature we invoke the equipartition theorem:  $\langle \psi_k \frac{\partial H}{\partial \psi_k} \rangle = T$ . Using Eq. (2) and summing over all lattice sites, it is readily verified that

$$T = \frac{1}{N} (\langle E_{\text{kin}} \rangle + 2 \langle E_{\text{int}} \rangle), \quad (3)$$

with  $E_{\text{kin}}$  and  $E_{\text{int}}$  being the kinetic and interaction energies [the first and second terms in the right-hand side of Eq. (2)]. The average is, for example, an average over the initial conditions. We find, however, that it is possible to accurately evaluate the temperature in a single run through the nonlinear medium provided that the lattice is large enough and that thermalization is established. The term  $E_{\text{int}}$  can be directly evaluated from the output field while  $E_{\text{kin}}$  can be evaluated from its Fourier transform. An alternative method to evaluate the effective temperature which is valid only for strong nonlinearity ( $|\Gamma| \gg 1$ ) is presented in [16] and yields identical temperatures. Finally we note that by properly choosing the initial conditions, we can change both  $\langle E_{\text{kin}} \rangle$  and  $\langle E_{\text{int}} \rangle$  and thus control the effective temperature  $T$ .

For any temperature it is possible to find  $|\Gamma| \gg 1$  such that  $\psi_i \psi_j^* + \psi_j \psi_i^* \approx 2 \cos(\theta_i - \theta_j)$  [17]. Using this approximation the Hamiltonian [Eq. (2)] decouples into two parts:

$$H_{\text{amplitude}} = \frac{1}{2} |\Gamma| \sum_{k=1}^N I_k^2, \quad (4)$$

$$H_{\text{phase}} = -2 \sum_{(i,j)} \cos(\theta_i - \theta_j). \quad (5)$$

$H_{\text{phase}}$  [Eq. (5)] is identical to the Hamiltonian of the 2D XY model, where for focusing nonlinearity the system is analogous

to an antiferromagnet and for defocusing nonlinearity to a ferromagnet. Both these Hamiltonians represent systems that undergo a Berezinskii-Kosterlitz-Thouless phase transition. In what follows we limit the discussion to defocusing nonlinearity corresponding to the ferromagnetic case. We also fix the value of  $\mu$  by working with constant input intensity.

Note, however, that since the DNLS Hamiltonian belongs to the XY universality class the strong nonlinearity limit is not required in order to observe the BKT phase transition. This is because the breakdown of long-range order is not due to the amplitude fluctuations which are increasingly suppressed as the temperature decreases.

#### IV. PHOTONIC BKT CROSSOVER

Having established the notion of a controllable effective temperature, we now explain how it facilitates the observation of the BKT transition. We simulate light propagating in a 2D nonlinear waveguide array employing a split-step fast Fourier method to solve Eq. (1). A square array of  $N = L \times L$  waveguides is simulated for various values of  $N$ , for a normalized propagation distance of  $\tilde{z} = 150$ , which we numerically verify to be larger than the thermalization length for all temperatures [16]. We use a nonlinear coefficient  $|\Gamma| = 50$ . The highest temperature is achieved using completely uncorrelated random phases at the input, and low temperatures were obtained by filtering the random phases with a low-pass filter with a controllable width (see [16] for a graph of the effective temperature as a function of the low-pass filter width). Typically we average over 32 different initial conditions.

A characteristic feature of the BKT phase transition is the profound change of the radial correlation function

$$C(r) = \iint_{r \leq \sqrt{x^2 + y^2} \leq r + dr} dx dy \langle \psi^*(x_0, y_0) \psi(x_0 + x, y_0 + y) \rangle, \quad (6)$$

where  $r$  is the radius, from algebraic decay below  $T_c$  to exponential decay above  $T_c$ . In the algebraic decay regime ( $T < T_c$ ) the correlation is given by  $C(r) \propto r^{-\alpha(T)}$  whereas in the exponential regime ( $T > T_c$ ) it is  $C(r) \propto \exp[-r/\xi(T)]$ . We simulated the propagation of light with partially random initial phase in a  $256 \times 256$  waveguide array for normalized temperatures in the range 0.6–1.5 and calculated the correlation function  $C(r)$  as a function of  $r$  directly from the correlation image, which is proportional to the Fourier transform of the far-field intensity profile of the output—see insets (a) and (b) of Fig. 1. We found that after three lattice sites (and up to the maximum  $\leq L/2$  lattice sites) the correlation function attained its universal form which is insensitive to the lattice discreteness. To differentiate between the two functional forms we employ two fits; a linear fit of  $\ln[C(r)]$  vs  $\ln(r)$  where a good fit indicates power-law decay, and  $\ln[C(r)]$  vs  $r$ , where a good fit indicates exponential decay. In practice, we had to include in the fit also a white noise floor (see [16] for sample fits from each type and for further details). In Fig. 1 we plot the linear regression goodness-of-fit parameter— $R^2$  for both fits. A clear transition from power-law behavior at low temperatures to exponential decay at higher temperatures

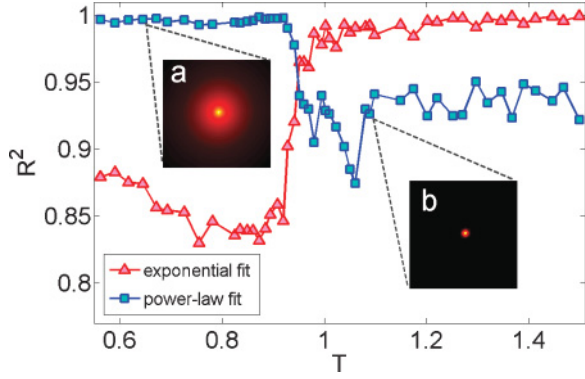


FIG. 1. (Color online) Linear regression goodness-of-fit parameter ( $R^2$ ) vs normalized temperature (both without units). In order to distinguish between the two types of correlation we used a linear fit of  $\ln[C(r)]$  vs  $\ln(r)$  where a good fit indicates power-law decay (blue squares), and a linear fit of  $\ln[C(r)]$  vs  $r$  where a good fit indicates exponential decay (red triangles). The transition occurs at  $T = 0.95 \pm 0.04$  in accordance with the known transition point  $T_c = 0.89$  [18]. Inset (a) is 2D correlation image at  $T < T_c$ . Inset (b) is the 2D correlation image at  $T > T_c$  (in both insets the intensity scale is logarithmic). For sample fits of  $C(r)$  vs  $r$  in log-log and semilogarithmic scale, see [16].

is observed at  $T = 0.95 \pm 0.04$  in accord with the known result [18].

While the previous method allows us to locate the transition temperature with good accuracy, the observable is not a physical quantity. A physical observable that facilitates the distinction between the two BKT phases is the cumulative integral of the radial correlation function  $\langle |A_Q|^2 \rangle$  [19] defined by

$$\langle |A_Q|^2 \rangle = \int d\vec{r} d\vec{r}_0 |\tilde{C}(\vec{r} - \vec{r}_0)|^2 \propto \Omega \int_0^{\sqrt{\Omega}} r dr |C(r)|^2, \quad (7)$$

where  $\vec{r} = (x, y)$ ,  $\vec{r}_0 = (x_0, y_0)$ ,  $\tilde{C}(\vec{r} - \vec{r}_0)$  is the Cartesian correlation function [integrand in Eq. (6)],  $\Omega$  is the integration area, and  $C(r)$  is the radial correlation function, defined in Eq. (6). Below  $T_c$  the correlation is algebraic  $C(r) \propto r^{-\alpha}$ ; therefore  $\langle |A_Q|^2 \rangle \propto \Omega^{2-\alpha}$ . Above  $T_c$  the correlation decays exponentially; hence for large enough  $\Omega$  the integral part of Eq. (7) will be constant and  $\langle |A_Q|^2 \rangle \propto \Omega$ . We therefore define the exponent  $\kappa(T)$  such that for all temperatures  $\langle |A_Q|^2 \rangle = \Omega^{2\kappa(T)}$ . By looking at  $\kappa$  as a function of the temperature  $T$ , the phase transition can be identified as a jump from  $\kappa = \frac{7}{8}$  just below  $T_c$  where  $\alpha_c = \frac{1}{4}$ , to  $\kappa = \frac{1}{2}$  just above  $T_c$  [19]. We note that for massive bosons at temperatures  $T < T_c$ ,  $2\pi[2 - 2\kappa(T)]$  is the inverse superfluid stiffness [18].

The function  $\langle |A_Q|^2 \rangle$  is calculated from the simulations by extracting the one-dimensional correlation function  $C(r)$  from the 2D correlation image (see inset figures in Fig. 1) and using Eq. (7). We then fitted  $\langle |A_Q|^2 \rangle$  to  $\Omega^{2\kappa}$ , thus extracting the scaling exponent  $\kappa$ . In Fig. 2 we calculate  $\kappa$  vs temperature for three lattice sizes ( $L = 64, 128,$  and  $256$ ). A rapid jump in the scaling exponent is apparent upon passing through the critical temperature  $T \approx 0.9$ . Also apparent is the sharpening of the crossover as the number of lattice sites increases, as expected. Note that at the critical temperature all three curves approximately meet.

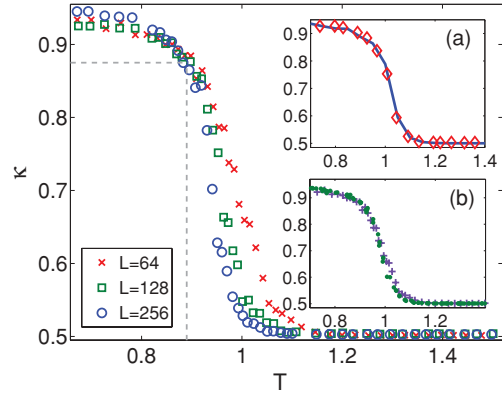


FIG. 2. (Color online)  $\kappa$  (no units) as function of normalized temperature (no units) for three lattice sizes. The dashed gray line corresponds to  $\frac{7}{8}$ , which is expected just below the phase transition. Inset (a): Comparison between extremely nonlinear waveguide propagation (red  $\times$ 's) and an XY Monte Carlo simulation (solid blue line) in a  $64 \times 64$  array. Inset (b):  $\kappa$  vs the effective temperature calculated either by averaging over propagation distance (green dots) or by initial condition averaging (purple plus signs) for a  $64 \times 64$  array. Good agreement between the two averaging methods is clearly observed.

To further consolidate the equivalence between the finite-size XY model and the nonlinear waveguide array, we repeat the simulation of the  $64 \times 64$  lattice but with four times stronger nonlinearity (i.e.,  $|\Gamma| = 200$ ) and then computed  $\kappa$  as a function of temperature. We then calculated the same  $\kappa$  dependence but using the XY model Hamiltonian instead [Eq. (5)]. We found very good agreement between the waveguide simulation and the XY model [inset (a) of Fig. 2]. Comparing the critical temperature obtained when  $|\Gamma| = 50$  to  $|\Gamma| = 200$ , we find a slight shift downward in the critical temperature when the nonlinearity is smaller, which is expected as the role of the intensity fluctuations is larger in this case.

Above the transition, free vortices start to proliferate as the breaking of vortex pairs decreases the free energy [18,21]. The average number of free vortices (calculated by numerically employing the Stokes theorem) is plotted in Fig. 3 as red circles. To fit this measurement we calculate the expected number of free vortices  $N_v(T)$  as follows. For temperatures

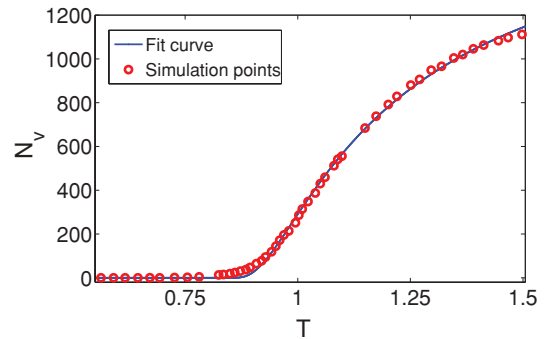


FIG. 3. (Color online) Average number of free vortices as a function of the normalized temperature (no units). Red circles, simulation results; solid blue line, theoretical fit.

above the transition temperature  $T > T_c$  the correlation length scales like  $\xi(T) \sim e^{B(T-T_c)^{-1/2}}$  where  $B$  is a constant that fixes the units. It follows that the number of free vortices,  $N_v(T)$ , scales as  $N_v(T) \sim \Omega \xi(T)^{-2}$ . We therefore fitted the average number of free vortices,  $N_v(T)$ , obtained from the simulations (red circles) to the function [18]

$$N_v(T) = A\theta(T - T_c)e^{-2B(T-T_c)^{-1/2}}, \quad (8)$$

where  $A$  and  $B$  are fit parameters that also fix the units and  $\theta(T - T_c)$  is the step function. We obtained a good fit as can be observed in Fig. 3. We note that by freeing  $T_c$  to be a fit parameter as well we obtain a critical temperature of  $T_c = 0.87 \pm 0.01$ , close to 0.89, which is the known transition temperature of the XY model. Incidentally, this formula might also prove useful for analyzing vortex proliferation in the context of ultracold atoms, both in simulations and in experiments [20,21].

As a possible experimental realization a large 2D waveguide array with sufficiently high Kerr nonlinearity is required [8,22,23]. The experimental setup would then consist of a coherent light source, an input imaging system injecting the light into the array, propagation in the nonlinear array, and an appropriate output imaging system. Control of the random initial condition can be readily achieved with the help of a computer-controlled spatial light modulator imaged over the waveguide array. At the output, a lens in a  $2f$  configuration can be used for example, to optically Fourier transform the output and image it onto a charge-coupled device (CCD). Taking the Fourier transform of the obtained CCD intensity profile thus yields the two-dimensional correlation function,

from which the radial correlation  $C(r)$  can be readily evaluated and therefore also the scaling of  $\langle |A_Q|^2 \rangle$  (Fig. 2). In addition, the total vorticity can be measured [24].

## V. CONCLUSIONS

To conclude, we showed that a periodic 2D waveguide array with Kerr-nonlinearity exhibits a Berezinskii-Kosterlitz-Thouless crossover associated with a vortex-unbinding transition. Thermal averaging was realized by averaging the output result over random initial conditions. By varying the initial energies we scanned the effective temperature and recreated important observables of the BKT transition, namely, the integrated correlation function and the average number of free vortices. Good agreement between the finite-size theoretical predictions and our simulations was found. The ability to define an analog to temperature in an all-optical setting can facilitate experiments on other interesting phase transitions known in condensed matter. For example, it would be interesting to study the role of the long-range (mean-field) interaction by globally coupling all the waveguides [25] or to study the antiferromagnetic ordering that is expected for focusing nonlinearity. In that case it is known that certain lattice structures (e.g., a Kagome lattice) can lead to frustration.

## ACKNOWLEDGMENTS

We would like to thank Ehud Altmann, Yoav Sagi, and Nir Davidson for helpful discussions and the Crown Photonics Center for support.

- 
- [1] V. L. Berezinskii, Zh. Eksp. Teor. Fiz **59**, 907 (1970) [Sov. Phys. JETP **32**, 493 (1971)].
  - [2] J. M. Kosterlitz and D. J. Thouless, J. Phys. C **5**, L124 (1972); **6**, 1181 (1973).
  - [3] D. R. Nelson and J. M. Kosterlitz, Phys. Rev. Lett. **39**, 1201 (1977).
  - [4] D. J. Bishop and J. D. Reppy, Phys. Rev. Lett. **40**, 1727 (1978).
  - [5] D. J. Resnick, J. C. Garland, J. T. Boyd, S. Shoemaker, and R. S. Newrock, Phys. Rev. Lett. **47**, 1542 (1981).
  - [6] J. Nielsen, J. D. Litster, R. J. Birgeneau, M. Kaplan, C. R. Safinya, A. Lindegaard-Andersen, and S. Mathiesen, Phys. Rev. B **22**, 312 (1980).
  - [7] Z. Hadzibabic *et al.*, Nature (London) **441**, 1118 (2006).
  - [8] F. Lederer *et al.*, Phys. Rep. **463**, 1 (2008).
  - [9] D. N. Christodoulides, F. Lederer, and Y. Silberberg, Nature (London) **424**, 817 (2003).
  - [10] A. Trombettoni and A. Smerzi, Phys. Rev. Lett. **86**, 2353 (2001).
  - [11] C. J. Pethick and H. Smith, Bose-Einstein Condensation in Dilute Gases (Cambridge University Press, Cambridge, 2002).
  - [12] O. Morsch and M. Oberthaler, Rev. Mod. Phys. **78**, 179 (2006).
  - [13] A. C. Cassidy, D. Mason, V. Dunjko, and M. Olshanii, Phys. Rev. Lett. **102**, 025302 (2009).
  - [14] R. Y. Chiao and J. Boyce, Phys. Rev. A **60**, 4114 (1999).
  - [15] R. K. Pathria *et al.*, Statistical Mechanics (Butterworth-Heinemann, Oxford, 2001).
  - [16] See supplemental material at [<http://link.aps.org/supplemental/10.1103/PhysRevA.83.013806>] for an alternative method to calculate the effective temperature in the strong nonlinearity limit, a figure of the effective temperature vs. the initial phase correlation width, a figure of the thermalization length vs. the effective temperature and sample fits of the correlation function above and below the BKT transition.
  - [17] Y. Silberberg, Y. Lahini, Y. Bromberg, E. Small, and R. Morandotti, Phys. Rev. Lett. **102**, 233904 (2009).
  - [18] P. M. Chaikin and T. C. Lubensky, Principles of Condensed Matter Physics (Cambridge University Press, Cambridge, 1995).
  - [19] A. Polkovnikov, E. Altman, and E. Demler, Proc. Natl. Acad. Sci., USA **103**, 6125 (2006).
  - [20] C. J. Foster, P. B. Blakie, and M. J. Davis, Phys. Rev. A **81**, 023623 (2010).
  - [21] V. Schweikhard, S. Tung, and E. A. Cornell, Phys. Rev. Lett. **99**, 030401 (2007).
  - [22] J. W. Fleischer *et al.*, Nature (London) **422**, 147 (2003).
  - [23] A. Szameit *et al.*, Opt. Express **14**, 6055 (2006).
  - [24] R. I. Egorov, M. S. Soskin, D. A. Kessler, and I. Freund, Phys. Rev. Lett. **100**, 103901 (2008).
  - [25] S. Gupta and D. Mukamel, Phys. Rev. Lett. **105**, 040602 (2010).